MONTE CARLO STUDIES OF MUON BACKGROUND AT SND@LHC

A.-G. Şerban*, R. Bruce, F. Cerutti, A. Donadon Servelle, S. Ilieva, B. Lindström, R. Cala'
CERN, Geneva, Switzerland

Abstract

The dominant background for neutrino signal at the SND@LHC experiment consists of muons reaching the detector after traversing several tens of meters of rock. Monte Carlo simulations were instrumental in the experiment design and the background study. For the latter, a two-step workflow was adopted, first simulating with FLUKA proton–proton collisions in ATLAS and recording secondary muons on a virtual interface plane in the rock, and then propagating them to SND@LHC with Geant4. Benchmarking of simulated integral fluxes against Run-3 measurements showed a level of agreement within 10–15% and enabled the interpretation of the significant variations that were observed as a function of the LHC optics and beam crossing plane. In particular, the role of diffractive proton losses in an accelerator cell upstream of the detector was highlighted. On this basis, effective mitigation strategies, such as orbit bumps displacing these losses to other cells, were explored. For the HL-LHC configuration of Run-4, first estimates indicate a significantly higher muon background than in Run-3, reflecting not only the planned luminosity increase but also the larger leakage due to the magnet aperture enlargement.

INTRODUCTION

The Scattering and Neutrino Detector at the LHC (SND@LHC) [1, 2] is a forward physics experiment located at 480 m from the ATLAS Interaction Point (IP1), in the TI18 tunnel. Designed to detect high-energy neutrinos (100 GeV–1 TeV) in the pseudo-rapidity region $7.2 < \eta < 8.4$ [3,4], the detector is shielded by roughly 70 m of rock and concrete along the ATLAS line-of-sight. In view of this shielding, long-range muons originating from proton–proton ($p-p$) collisions in IP1 constitute the primary background for neutrino interaction searches. These muons can escape the veto system and induce showers, mimicking neutrino signals. In addition, the sustained muon flux gradually saturates the emulsion target, necessitating periodic replacements during data-taking. A comprehensive characterization of the muon flux through measurements and Monte Carlo (MC) simulations is therefore essential. This work presents the evolution, interpretation, and mitigation of the muon background across the various LHC configurations during Run-3 (2022–2026), and provides an outlook for the High-Luminosity LHC (HL-LHC) era in Run-4 (2030–2033).

MC SIMULATION WORKFLOW

The SND@LHC muon background is simulated using a two-step approach. First, $p-p$ collisions at center-of-mass energies of $\sqrt{s} = 13.6$ TeV (Run-3) and 14 TeV (Run-4) are sampled with the DPMJET-III event generator [5, 6], embedded in FLUKA [7–9]. The resulting collision debris is transported through a detailed FLUKA geometry of the LHC tunnel, extending from the ATLAS cavern to a virtual interface plane 30 m upstream of SND@LHC. At this plane, the kinematics, statistical weight, and production history of each muon are recorded. Second, a Geant4 [10] simulation propagates these muons from the interface plane through the upstream rock and the SND@LHC detector, accounting for secondary particle production. Benchmarking of the MC simulated muon rate against experimental measurements at SND@LHC was performed for all Run-3 configurations, yielding a good agreement, as reported in the following section.

MUON BACKGROUND ACROSS RUN-3

The experimental muon rates, Φ_{exp}, at SND@LHC during Run-3, alongside their corresponding MC estimates, Φ_{MC}, are summarized in Table 1. Their level of agreement is quantified by the relative difference δ, defined as:

$$\delta = \frac{\Phi_{\text{MC}} - \Phi_{\text{exp}}}{\Phi_{\text{exp}}}, \tag{1}$$

where

$$\Phi_{\text{MC}} = \frac{\sum_{i=1}^{N_{\text{tracks}}} w_i}{N_{p-p}} \times \sigma_{\text{inel}} \times \mathscr{L}. \tag{2}$$

The number of simulated $p-p$ collisions (of the order of 50 to 100 million) is denoted by N_{p-p}, the number of muons reconstructed within the active volume of the detector is N_{tracks}, while w_i represents their statistical weight. The inelastic $p-p$ cross-section at $\sqrt{s} = 13.6$ TeV (including diffractive events) is $\sigma_{\text{inel}} \approx 80$ mb and the reference Run-3 instantaneous luminosity is $\mathscr{L} = 2 \times 10^{34}$ cm^{-2} s^{-1}. Despite the complexity of the multi-step simulation framework, the MC predictions are in good agreement with the measurements across all Run-3 configurations and reflect their significant variations.

These variations are driven by the machine optics and beam crossing scheme adopted in Insertion Region 1 (IR1), which hosts the ATLAS experiment. In 2022–2023, the LHC operated in IR1 with downward vertical crossing (VC, −160 µrad half-crossing angle) and nominal optics, employing a focusing-defocusing-focusing[1] (FDF) sequence for the Q1, Q2, and Q3 final-focus quadrupoles. This configuration yielded the lowest muon rate recorded during Run-3. To redistribute the impact of collision debris on the aforementioned quadrupoles, the 2024 run operated with upward VC

* alexandra.serban@cern.ch

[1] The focusing/defocusing effect applies to the outgoing proton beam in the horizontal plane.

Table 1: LHC configurations and corresponding muon rates at SND@LHC during Run-3, normalized to $\mathscr{L} = 2 \times 10^{34}$ cm^{-2} s^{-1}. Statistical uncertainties are given for both measurements and MC estimates.

Year	**IP1 crossing**	**Beam optics**	**Muon rate (Hz)**		δ
			Φ_{exp}	Φ_{MC}	
2022–2023	Downward VC	Nominal	557 ± 1	500 ± 17	−10%
2024	Upward VC	RP	1154 ± 2	1008 ± 35	−12.5%
2025–2026	HC	Nominal	799 ± 1	907 ± 40	+13.5%

(+160 µrad) and a reverse-polarity (RP) optics [11], featuring an inverted DFD sequence for Q1–Q3 and Q4 switched off. The RP optics induced a twofold increase of the muon background at SND@LHC: the inverted DFD sequence augmented the flux of energetic (> 1 TeV) positive muons from the decay of particles generated in primary collisions at IP1, while larger diffractive proton losses in the dispersion suppressor (DS) enhanced the population of low-energy negative muons. To limit peak dose accumulation in the magnet coils, while addressing the 2024 background increase, the 2025 operation reverted to nominal optics in IR1, implementing for the first time horizontal crossing (HC). This partially mitigated the background but did not restore the 2022–2023 baseline, for the reasons explained below. The 2025 optics and crossing scheme are preserved for 2026.

MUON BACKGROUND MITIGATION

In 2025, measurements revealed an excess in the muon angular distribution at large positive angles (20–60 mrad) compared to 2022–2023, as shown in Fig. 1. MC simulations traced this excess to negative muons from nuclear inelastic interactions of diffractive protons lost in the second main dipole of half-cell 11, located 400 m from IP1, which are then bent towards SND@LHC by the dipole field. HC in IP1 maximizes such DS losses, making this muon population a sizeable background contributor in 2025[2]. Mitigation strategies focused on displacing these proton losses led to the conception and experimental validation of two orbit bumps [12]: a 9 mm downstream bump, shifting the losses from half-cell 11 into half-cells 13 and 15, and an 8 mm upstream bump, moving them into cell 8-9. The muon rates measured at SND@LHC during the orbit bump tests and the respective MC predictions are reported in Table 2. The downstream bump achieved a 20% decrease in the measured muon rate at the detector, while the upstream bump resulted in a 15% reduction. In both cases, the MC simulation underestimates the measured rates due to a local FLUKA overestimation of diffractive proton losses in half-cell 11 by approximately a factor of 2, causing the simulated reduction to exceed the measured one. The effect of the orbit bumps is apparent in Fig. 2, where the large positive-angle component due to negative muons from the DS vanishes with the displacement of diffractive proton losses away from half-cell 11.

Despite the success of these tests, no orbit bump was retained for 2026 due to its limited target integrated luminosity.

[2] As already in 2024 with RP optics and VC.

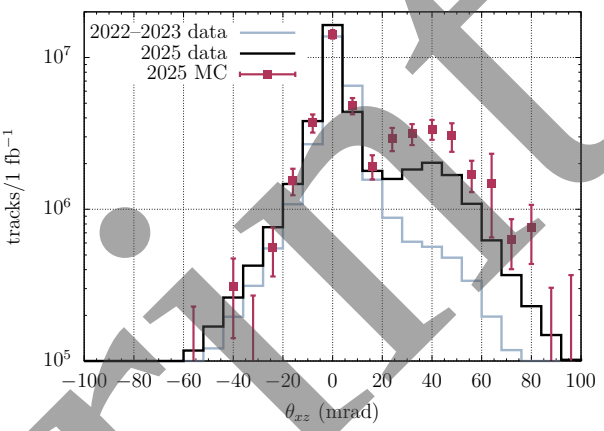

Figure 1: Angular distribution of muon tracks as measured in 2022–2023 (grey) and 2025 (black), and resulting from the 2025 MC simulation (red squares).

Table 2: SND@LHC muon background during the orbit bump tests: measured and simulated rates at $\mathscr{L} = 2 \times 10^{34}$ cm^{-2} s^{-1}, with respective statistical uncertainties and percentage differences.

	Downstream bump	**Upstream bump**
Φ_{exp} (Hz)	634 ± 24	666 ± 27
Φ_{MC} (Hz)	476 ± 24	534 ± 25
δ	−25%	−20%

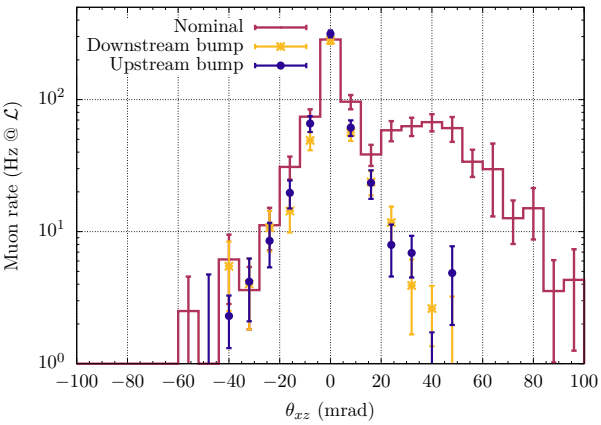

Figure 2: Simulated muon angular distribution for the 2025 configuration (red) and the downstream (yellow stars) and upstream (blue circles) orbit bump tests.

PROSPECTS FOR THE HL-LHC ERA

Following the HL-LHC upgrade, operation resuming in 2030 aims for a final target integrated luminosity of 3000 fb^{-1} within slightly more than a decade [13] by raising the instantaneous levelled luminosity in ATLAS and CMS to 5×10^{34} $cm^{-2}s^{-1}$. For SND@LHC, the transition to Run-4 brings a substantial increase in both signal and background, whose relative evolution is being carefully characterized.

A new FLUKA geometry was developed for the HL-LHC configuration (v1.5), incorporating the updated IR1 layout. At the aforementioned nominal HL-LHC instantaneous luminosity, the predicted muon rate at SND@LHC reaches 3345 Hz. Rescaled to the Run-3 instantaneous luminosity of 2×10^{34} $cm^{-2}s^{-1}$, this yields 1338 Hz, exceeding the 1154 Hz maximum recorded during the 2024 RP-optics run. Considering that HL-LHC will instead feature nominal triplet polarity (and HC in IR1, as in 2025–2026, but with the magnitude of the half-crossing angle increased from 160 to 250 µrad), the predicted background rise reflects the significant layout changes to be implemented by 2030. In particular, the new final-focus quadrupoles have a coil aperture of 150 mm in diameter, more than twice that of the current Q1–Q3 (70 mm). The same applies to the new superconducting separation dipole D1, which will replace the present normal-conducting one having a vertical aperture of 63 mm, as depicted in Fig. 3. The effect of these enlarged apertures was quantified in a dedicated MC simulation, where the new Q1–D1 string aperture in the HL-LHC FLUKA geometry was artificially reduced back to 70 mm, yielding a factor of 2 reduction in the muon rate at SND@LHC.

Diffractive proton losses in the IR1 DS are expected to persist in Run-4, driven by the HC plane foreseen in the HL-LHC baseline configuration for ATLAS. Therefore, orbit bumps, analogous to the ones successfully tested in 2025, remain a promising mitigation measure for reducing the population of large-angle low-energy muons. On the other hand, muons produced by collision debris interactions with machine elements along the straight section are harder to mitigate. Nonetheless, SND@LHC data-taking is not expected to be hindered. In fact, a key limitation during Run-3 was the sensitivity of emulsion films to track accumulation, requiring regular replacements. The planned upgrade to silicon vertex detectors [14] removes this constraint, making Run-4 operation viable even at elevated background levels. It shall be noted that the possible adoption of a VC scheme in IR1 would provide a ~20% reduction in muon background relative to the horizontal baseline, although its implementation would require relocating the crab cavities between the ATLAS and CMS insertions.

CONCLUSIONS

The muon background at SND@LHC has been characterized across the full Run-3 period through direct measurements and combined FLUKA–Geant4 simulations, yielding agreement within 10–15% for the operational configurations and 20–25% for the orbit bump tests. The SND@LHC muon flux proved highly sensitive to the LHC optics and beam crossing configurations in Insertion Region 1. In 2024, a twofold increase was observed due to the reverse-polarity optics. The subsequent restoration of nominal optics paired with horizontal crossing reduced the 2025 background, but did not restore the 2022–2023 levels, owing to negative muons from diffractive proton losses in half-cell 11 of the dispersion suppressor, as unveiled by simulations. Orbit bumps displacing these losses either upstream or downstream achieved measured background reductions of 15% and 20%, respectively. For HL-LHC, simulations predict a fourfold increase in the muon rate at the future nominal instantaneous luminosity compared to 2025, reflecting not only the higher collision rate but also the significantly enlarged apertures of the final-focus quadrupoles and separation dipole. Nevertheless, the planned transition to silicon vertex detectors is expected to enable the efficient operation of SND@LHC even at such an elevated background level.

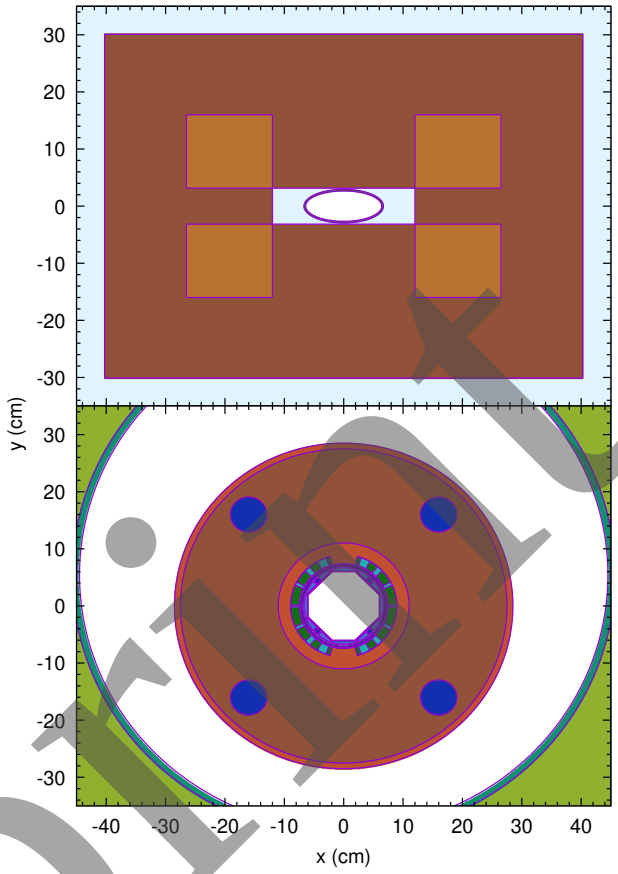

Figure 3: Transverse section of the LHC (top) and HL-LHC (bottom) separation dipoles as modelled in FLUKA.

ACKNOWLEDGEMENTS

The authors thank S. Fartoukh for his leading role in the elaboration of the different LHC configurations, V. Rodin for their setup in FLUKA, the LHC operation team for the implementation of the orbit bumps, and M. Sabaté Gilarte and D. Prelipcean for the FLUKA model of HL-LHC.

REFERENCES

[1] G. Acampora *et al.*, "SND@LHC: the scattering and neutrino detector at the LHC", *J. Instrum.*, vol. 19, p. 05067, 2024. doi:10.1088/1748-0221/19/05/P05067

[2] D. Abbaneo *et al.*, "Installation and performance of the 3rd Veto plane at the SND@LHC detector", *J. Instrum.*, vol. 20, 2025. doi:10.1088/1748-0221/20/07/P07011

[3] R. Albanese *et al.*, "Observation of Collider Muon Neutrinos with the SND@LHC Experiment", *Phys. Rev. Lett.*, vol. 131, p. 031802, 2023. doi:10.1103/PhysRevLett.131.031802

[4] D. Abbaneo *et al.*, "Observation of Collider Neutrinos without Final State Muons with the SND@LHC Experiment", *Phys. Rev. Lett.*, vol. 134, p. 231802, 2025. doi:10.1103/r2qy-9hft

[5] S. Roesler, R. Engel, and J. Ranft, "The Monte Carlo event generator DPMJET-III", in *Proc. Int. Conf. Advanced Monte Carlo for Radiation Physics, Particle Transport Simulation and Applications*, Lisbon, Portugal, Oct. 2000, pp. 1033–1038. doi:10.1007/978-3-642-18211-2_136

[6] A. Fedynitch, "Cascade equations and hadronic interactions at very high energies", PhD Thesis, Karlsruhe Institute of Technology, 2015. https://cds.cern.ch/record/2143091

[7] "Fluka website", https://fluka.cern,

[8] C. Ahdida *et al.*, "New Capabilities of the FLUKA Multi-Purpose Code", *Front. Phys.*, vol. 9, 2022. doi:10.3389/fphy.2021.788253

[9] G. Battistoni *et al.*, "Overview of the FLUKA code", *Annals Nucl. Energy*, vol. 82, pp. 10–18, 2015. doi:10.1016/j.anucene.2014.11.007

[10] S. Agostinelli *et al.*, "Geant4—a simulation toolkit", *Nucl. Instrum. Methods Phys. Res. A*, vol. 506, pp. 250–303, 2003. doi:10.1016/S0168-9002(03)01368-8

[11] G. Arduini *et al.*, "LHC Triplet Task Force Report", CERN, Geneva, Rep. CERN-ACC-2023-0004, 2023. https://cds.cern.ch/record/2882512

[12] A. Donadon Servelle *et al.*, "Mitigation of muon backgrounds at LHC forward-physics experiments through orbit bumps", presented at the 17th Int. Particle Accelerator Conf. (IPAC'26), Deauville, France, May 2026, paper THP4105, this conference.

[13] L. Rossi *et al.*, "The High Luminosity LHC, Technical Design Report", CERN, Rep. CERN-2020-010, 2020. doi:10.23731/CYRM-2020-0010

[14] D. Abbaneo *et al.*, "SND@HL-LHC, Scattering and Neutrino Detector in Run 4 of the LHC", CERN, Geneva, Rep. CERN-LHCC-2025-004, LHCC-P-026, 2025. https://cds.cern.ch/record/2926288